



# Magnetic resonance and antiresonance in microwave transmission through nanocomposites with Fe<sub>3</sub>Ni<sub>2</sub> and FeNi<sub>3</sub> particles



A.B. Rinkevich<sup>a</sup>, M.I. Samoylovich<sup>b</sup>, O.V. Nemytova<sup>a,\*</sup>, E.A. Kuznetsov<sup>c</sup>

<sup>a</sup> M.N. Miheev Institute of Metal Physics Ural Branch of RAS, 18 S.Kovalevskaya St, Ekaterinburg 620990, Russia

<sup>b</sup> OAO TsNITI "TEKHNOMASH", 4 Ivana Franko St, Moscow 121108, Russia

<sup>c</sup> Nizhny Tagil branch of the Ekaterinburg state social-pedagogical university, 57 Krasnogvardeyskaya St, Nizhny Tagil 622031, Russia

## ARTICLE INFO

### Article history:

Received 27 July 2016

Accepted 27 January 2017

Available online 22 February 2017

### Keywords:

Opal matrices

Nanocomposite materials

Microwave properties

Magnetic resonance and antiresonance

## ABSTRACT

Investigation of magnetic properties and microwave resonance phenomena in nanocomposites based on opal matrices containing the particles of intermetallide of Fe<sub>3</sub>Ni<sub>2</sub> and FeNi<sub>3</sub> is carried out. The interactions which lead to the resonance changes of transmission and reflection coefficients are determined. Electromagnetic properties are measured in the millimeter frequency range. Special attention is paid to comparison between static and dynamic magnetic properties of nanocomposites. Frequency dependences of magnitude of lines of resonance features are obtained. Spectra of resonance and antiresonance are studied. The conditions when the magnetic antiresonance is observed are clarified. The X-ray phase analysis of the nanocomposites is performed and their structure is studied.

© 2017 Elsevier B.V. All rights reserved.

## 1. Introduction

### 1.1. Anomalies of physical properties of nanocomposite materials based on opal matrices

Nanocomposite materials based on opal matrices have become the topical exploration subject. Due to the periodical structure these materials can be considered either as the metamaterials [1] or as the photonic crystals [2], depending on the chemical composition and frequency range of the electromagnetic waves. Physical properties and structure of the opal matrices filled by the metallic or ferromagnetic nanoparticles have been studied in detail in [3]. There are some prospects of application of nanocomposite based on the opal matrices as the magnetic metamaterials in the nano-electronic devices of microwave frequency range [4].

Microwave techniques enable relatively easy to estimate the dynamic and relaxation parameters of such materials. Opal matrices with the embedded magnetic metallic nanoparticles can be considered as the metamaterials which are suitable to create the media with a negative refractive index [5]. Realization of such left-handed medium with the negative real part of magnetic permeability is possible, in the first place, in the region of magnetic resonances. At the resonance field the sign of dynamic magnetic permeability changes and its value can considerably vary. In the

work [6] the conditions of realization a negative refractive index in the case of nanocomposite material based on opal matrix filled with the conductive ferromagnetic nanoparticles have been achieved. There are the conditions under which the metamaterials have permeability close to zero. In such media there is a tunnelling effect through the narrow channels and bends under the conditions when the normal transmission of wave is not permitted [7–9].

Microwave properties of 3D-nanocomposites based on opal matrices depend on their phase composition and magnetic state. An influence of contribution of nanoparticles surface to the magnetic anisotropy is typical for the magnetic properties of nanoparticles. As well as the processes of superparamagnetic relaxation are important [10,11]. The magnetic state of nanocomposite is a factor which defines the microwave properties in magnetic field, in particular, the resonance phenomena.

The dynamics of magnetization under the resonance conditions is carefully studied. Investigation of several parameters, namely, the value of attenuation of electromagnetic waves, spectrum of magnetic resonance and linewidth is required to correctly describe and understand the processes of wave's interaction with magnetic 3D-nanocomposites. Characteristics of resonance line such as the value of field of resonance, the width and shape of line, depend on the size of nanoparticles [12].

The greatest changes of transmission and reflection coefficients of electromagnetic waves in microwave and millimeter-wave bands take place due to the influence of magnetic resonance and

\* Corresponding author.

E-mail address: [mif-83@mail.ru](mailto:mif-83@mail.ru) (O.V. Nemytova).

antiresonance. Ferromagnetic resonance (FMR) leads to the electromagnetic waves absorption which as usual leads to a minimum in the field dependence of reflection and transmission coefficients. Ferromagnetic antiresonance (FMAR) is realized by changing the sign of permeability of metallic ferromagnet in the fields which are less than the field of uniform mode of magnetic resonance [13]. The antiresonance occurs when the real part of permeability equals zero and the imaginary part is small. Mostly the antiresonance is experimentally observed as anomalous transmission of electromagnetic wave through the ferromagnetic film, which occurs because of considerable increase of skin depth [14]. Theoretical description of antiresonance is given in [15].

Magnetic resonance and antiresonance are observed in the magnetic nanowires of FeCoNi obtained by electro deposition, followed by magnetron sputtering [16]. The distance upon which the wave is attenuated in the film of Fe of 3  $\mu\text{m}$  in thickness, deposited on the dielectric substrate, is calculated in [17]. The control of transparency of film nanocomposites of ferrite – carbon is achieved in the region of FMR and FMAR on microwaves in paper [18].

When changing the frequency or intensity of magnetic field, there is a point where the real part of the dynamic magnetic permeability vanishes in any ferromagnetic or ferrimagnetic media. In the case of conductive medium, an influence of change of skin depth is predominant. Under the antiresonance condition the skin depth significantly rises and the increase of transmission coefficient mentioned above is observed. In the nonconductive media other manifestation of magnetic antiresonance takes place. In such media the skin effect is absent, but the surface or input impedance as well as absorption coefficient of electromagnetic wave change. The magnetic resonance and antiresonance in nanocomposite based on the opal matrixes was observed in [20].

Using the appropriate elements of microwave technique and realizing various schemes of measurement, it is possible to realize different mutual orientation of the microwave field and external magnetic field. Thus the conditions of most effective interaction of nanoparticles of introduced substance with fields can be achieved. The peculiarities of transmission and reflection coefficients which are caused by magnetic resonance are more clearly pronounced upon the perpendicular orientation of constant  $H$  and microwave  $H_{\sim}$  magnetic fields,  $H \perp H_{\sim}$  [13]. Upon  $H \parallel H_{\sim}$  the peculiarities of transmission, reflection, absorption, related to FMR, is not observed. This fact is well known, for instance, for thin homogeneous ferromagnetic films.

In this paper the microwave resonance phenomena in nanocomposites based on the opal matrixes with the nanoparticles of iron and nickel intermetallides placed into the interspherical voids are investigated. All of these introduced compounds are ferromagnetic, but their magnetic properties are different from each other. Microwave properties have been measured at the frequencies of millimeter waveband. The microwave signal transmitted through the nanocomposite changes, in general, due to the change of surface impedance of nanocomposite under magnetic resonance condition and the absorption of electromagnetic wave. Magnetic resonance phenomena in nanocomposites and their influence on the reflection and transmission coefficients through the nanocomposite are studied. Special attention is paid to comparison of static and dynamical magnetic properties of the nanocomposites. The conditions of occurrence of magnetic antiresonance are elucidated. The techniques of measurement of transmission and reflection coefficients of waves are used in microwave measurement [21,22]. The frequency range from 26 to 38 GHz is used for the following reason. Firstly, the electromagnetic wave frequency must be large enough to the effect the magnetic antiresonance could be observed [13]. The minimum frequency is determined by the magnetization of studied material. Secondly, it is desirable that the field of magnetic resonance would be corresponding to satu-

rated magnetic state. The frequency dependences of magnitude of lines of resonance features are obtained and the spectra of FMR and FMAR are studied in this work.

Analysis of the results is carried out taking into consideration the phase composition, structure and magnetic state of the materials. The implementation of effective interaction of microwave fields with intermetallide nanoparticles is of interest both for finding the conditions of existence of negative real part of permeability, as well as for using in the electronic devices of microwave frequencies.

## 2. Structure and phase composition of nanocomposites with the intermetallide particles

### 2.1. Synthesis

Synthesis of samples of opal matrixes with the diameters of submicron amorphous  $\text{SiO}_2$  spheres ranging from 240 to 270 nm has been described elsewhere [23]. Nanocomposites with the embedded nanoparticles of oxides of transition metal were prepared by the impregnation technique with subsequent heat treatment. The properties of nanocomposite materials to a great extent depend on the technology of their production. The samples of opal matrixes were obtained by using the following technology. At the initial stage submicron spheres of amorphous  $\text{SiO}_2$  were produced according to the technology based on the reaction of hydrolysis of tetraether of orthosilicic acid  $\text{Si}(\text{OC}_2\text{H}_5)_4$  with a solution of ethanol  $\text{C}_2\text{H}_5\text{OH}$  with the presence of ammonium hydroxide  $\text{NH}_4\text{OH}$ , which served as a catalyst. At first, small branched nanoparticles have been formed. Then, during polycondensation, they transformed into spherical particles of amorphous silicon dioxide. After settling suspension and removing the hydrolyzate, an ordered precipitate represented a hydrogel containing a liquid (50–60 wt%). If additional measures don't be assumed that after drying the obtained material is chalk-like and readily broken. Therefore, in order to strengthen the obtained opal matrixes and remove unbounded water a posterior heat treatment was performed. Before impregnation of nanoparticles into the interspherical voids the opal matrix has close-packed periodic structure of submicron spheres. The regularity of the nanosphere packing was controlled using the shape and linewidth of the Bragg reflections.

Impregnation method is one of the easiest ways to introduce various chemical elements and compounds inside the opal matrixes. The method is based on the impregnation of the opal matrix by the precursor material with a specific chemical composition, followed by heat treatment, during which the desired chemical composition is formed in the interspherical voids. The precursor materials should have a good solubility in water (or in other solvents) and change into oxides (or other compounds) at moderate temperatures during heat treatment. In this work the soluble salts (nitrate) of metals have been used as the precursors. The procedure was repeated many times (up to 20 impregnations), so that the interspherical voids of the opal matrix were gradually filled. Next, the heat treatment is performed under the temperature ranging from 500 to 750 °C. During heat treatment the partial thermal decomposition of nitratogroups occurs and the unbound water is removed.

After deposition the particles of introduced substance are metal oxides. To obtain the nanocomposite with the metallic particles the sample were annealed in a hydrogen atmosphere at the temperature from 600 to 700 °C. Annealing conditions was following: 1) pumping air; 2) heating with the following desorption from sample (starts at 100–200 °C); 3) after completing of desorption the hydrogen pressure is increased up to 2.5 atm. Desorption was observed up to the temperature of 600 °C; 4) Annealing was carried out for

7 h at the temperature of 600–700 °C, at that more active decrease of hydrogen pressure was observed during the first hour.

In this work the intermetallides containing iron and nickel in various proportions are considered, therefore to prepare different intermetallide the various ratios of metal ions have been chosen. As a result, the nanocomposites with the particles of  $\text{Fe}_3\text{Ni}_2$  intermetallide and particles of  $\text{FeNi}_3$  intermetallide were prepared. The samples with the particles of  $\text{FeNi}_3$  differ from each other by the number of impregnation and temperature of heat treatment. The following notation of samples is used in this work: the numbers before slash indicate the serial number of sample, the numbers after slash indicate the number of impregnation, and the numbers after dash indicate the annealing temperature in hydrogen. For example, the notation of sample No.112/9-725 means: serial number is 112, sample was obtained with 9 impregnations, the annealing temperature was 725 °C.

The structure of sample No.112/9-725 with the nanoparticles of  $\text{FeNi}_3$  is shown in Fig. 1. Image was obtained by using the scanning

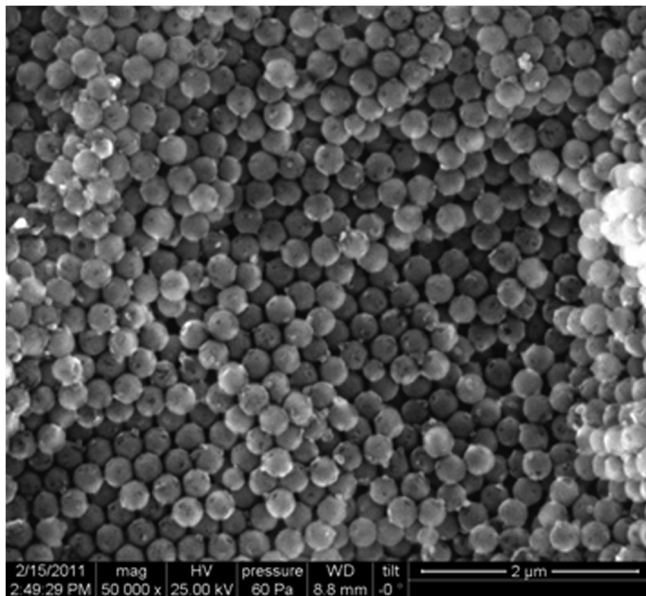


Fig. 1. The structure of sample No.112/9-725 with  $\text{FeNi}_3$  nanoparticles with the magnification of  $\times 60,000$ , obtained by using the scanning electron microscope of Quanta-200.

electron microscope of Quanta-200 with the magnification of  $\times 60,000$ . The particles of embedded phases have irregular shape and the dimensions from 10 to 60 nm. As it can be seen from Fig. 1, introduced substance is mostly contained in the interspherical voids. The volume concentration of introduced substance is from 5 to 15%.

X-ray phase analysis or X-ray diffraction (XRD) of incorporated substance was implemented by using diffractometer DRON 3 M with  $\text{CuK}_\alpha$ -radiation, flat graphite monochromator, upon rotation of sample either with the step of  $0.02^\circ$  or continuously with the rate of  $1^\circ$  per minute.

As the example, the X-ray diffraction pattern of nanocomposite sample No.112/9-725 of opal matrix with the compounds based on the Fe and Ni synthesized into nanovoides is shown in Fig. 2. X-ray analysis allows one to determine the presence of  $\text{FeNi}_3$  phase – cubic crystal system, space group Pm-3 m (38-0419). The XRD pattern shown in Fig. 2 contains sharp peaks of intensity which belong to the introduced crystalline phase, as well as a broad maximum in the angular range from 150 to 270 presents which is caused by the presence of  $\text{SiO}_2$  amorphous nanospheres. X-ray analysis of the sample No.413/6-650 allows one to determine the presence of following phase: probably,  $\text{Fe}_3\text{Ni}_2$  – cubic crystal system, space group Fm-3 m (65-5131). It is also found that the particles of incorporated substances in the samples No.414/6-650, No.480/5-700 and No.112/9-725 contain  $\text{FeNi}_3$  intermetallide. The sample No.413/6-650 contains the nanoparticles of  $\text{Fe}_3\text{Ni}_2$  intermetallide.

### 3. Magnetic properties of nanocomposites

It is well known that the magnetic properties of nanoparticles significantly differ from the properties of bulk material. Nanoparticles as well as 3D- nanocomposites are characterized by the influence of contribution of surface of nanoparticles to the magnetic anisotropy and the processes of superparamagnetic relaxation are important [24]. Microwave properties of ensembles of nanoparticles strongly depend on the method of preparation as well as their structure. The existence of magnetic forces between the particles is one of the reasons of ability of iron particles to form particle aggregates [25].

The purpose of this section is the systematic study of magnetic properties of magnonic crystals based on the opal matrices with the nanoparticles of  $\text{FeNi}_3$  and  $\text{Fe}_3\text{Ni}_2$  intermetallides into the interspherical areas. Magnetization curves and hysteresis loops will be measured.

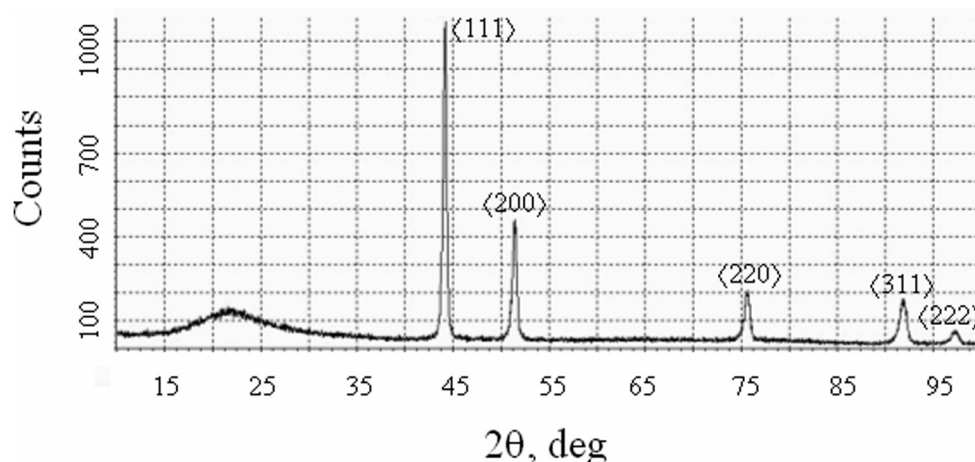


Fig. 2. X-ray diffraction pattern of nanocomposite sample No.112/9-725 of opal matrix with the compounds based on Fe and Ni synthesized in nanovoides, where (abc) are Miller indexes.

The magnetic measurements were carried out using the MPMS-XL instrument from Quantum Design at the temperature of 300 K in the field range up to 15 kOe as well as using the vibration magnetometer of Lake Shore company, model 7409. The region of magnetic field close to the condition of magnetic resonance is attended in this work. Therefore, the magnetization curve of nanocomposites is of the greatest interest as the magnetization value determines the field of magnetic resonance.

As a rule, exact quantity of magnetic phase introduced into the sample isn't known. Therefore, to obtain the magnetization the value of magnetic moment of sample should be attributed to the mass of entire sample. At that the sample-averaged magnetization is obtained. As the quantity of magnetic phase into the sample is indefinite it is incorrectly to compare the absolute value of magnetization for different samples. It can be compared the value of coercive force, saturation field, ratio of remanent magnetization to the saturation magnetization, the shape of magnetization curve and hysteresis loop.

Fig. 3 shows the hysteresis loop measured for studied samples at the temperature of 300 K. In this figure the sample number corresponds to the particular notation of sample according Table 1, column 1 and 2.

The information about magnetic properties of the studied samples of nanocomposites at room temperature is shown in Table 1. Also in this table in column 4 the estimated dimension of coherent-scattering region obtained from XRD measurement is indicated for all studied sample. All samples have sufficiently narrow hysteresis loop with the coercivity from 69 to 199 Oe. The saturation magnetization for different samples is different for the reasons mentioned above. It can be noted a significant difference between the sample No.413/6-650 with  $\text{Fe}_3\text{Ni}_2$  intermetallide and other samples which contain the particles of  $\text{FeNi}_3$  intermetallide. This distinction is probably related to the difference in Curie temperature of intermetallides. The change of Curie temperature  $T_C$  of Fe-Ni alloys subject to the concentration of Ni is considered

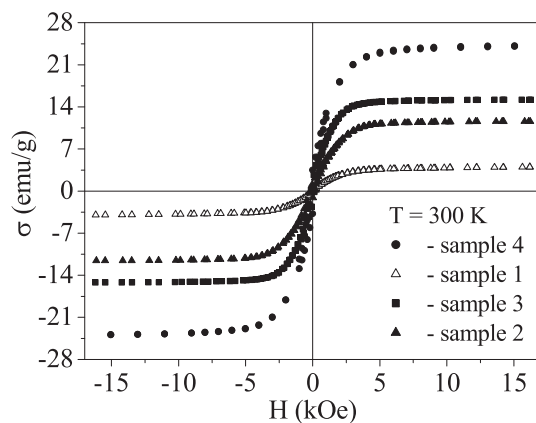


Fig. 3. The hysteresis loops measured for studied samples at the temperature of 300 K.

Table 1

The comparison of magnetic properties of samples, T = 300 K.

The sample number	The notation of sample	Composition of the introduced particles	The size of coherent-scattering region, nm	$M_s$ , emu/g	$M_r$ , emu/g	$M_r/M_s$	$H_c$ , Oe
1	2	3	4	5	6	7	8
1	413/6-650	$\text{Fe}_3\text{Ni}_2$	37.9–55.9	4.01	0.192	0.048	69
2	480/5-700	$\text{FeNi}_3$	25.1–40.1	11.58	1.25	0.104	199
3	414/6-650	$\text{FeNi}_3$	20.0–22.2	15.21	1.63	0.108	145
4	112/9-725	$\text{FeNi}_3$	20.7–24.2	24.3	3.3	0.123	121

in work [25]. Actually, at 40 at.% of Ni, which corresponds to  $\text{Fe}_3\text{Ni}_2$  composition,  $T_C \approx 650$  K, and for  $\text{FeNi}_3$  composition  $T_C \approx 910$  K. For sample No.413/6-650 the coercive force is significantly less than for other samples (69 Oe as compared to 121–199 Oe). The saturation magnetization  $M_s$  and the remanent magnetization  $M_r$  for this sample is also lower than for the others. It can be concerned both with the magnitude of magnetization of introduced phase and with the volume fraction of ferromagnetic nanoparticles in nanocomposite. The  $M_r/M_s$  ratio characterizes the degree of closeness of loop to the rectangular shape. The larger the  $M_r/M_s$  ratio, the closer the loop to the rectangular shape. It can be seen from the Table 1, that all hysteresis loops are far from rectangular shape, as  $M_r/M_s \ll 1$ . For samples with the  $\text{FeNi}_3$  nanoparticles there is a correlation – when increasing the impregnation number, the  $M_r/M_s$  ratio increases and the coercivity reduces.

#### 4. Microwave resonance properties of nanocomposites with the particles of intermetallide

##### 4.1. Microwave resonance properties of nanocomposites with the particles of $\text{Fe}_3\text{Ni}_2$ intermetallide

Nanocomposite materials are often prepared to study and applied them at the microwave frequencies. In [19] the microwave and magnetic properties of 3D-nanocomposites based on the opal matrices with the particles of nickel-zinc ferrite are studied. Special attention is paid to the magnetic resonance and antiresonance phenomena. The electromagnetic properties of nanoparticles of ferrite spinel  $\text{Co}_x\text{Mn}_{1-x}\text{Fe}_2\text{O}_4$  in paraffin have been investigated in the frequency range of 8–20 GHz [26]. The frequency dependences of permittivity and permeability have been studied in our paper. Microwave measurements are carried out in the frequency range from 26 to 38 GHz using the conventional rectangular waveguides operating at the  $\text{TE}_{10}$  mode. At whole frequency range single-mode operation is accomplished. To perform the microwave measurements the sample is placed into the waveguide with lateral dimensions of  $7.2 \times 3.6$  mm across the microwave circuit, see Fig. 4.

External DC magnetic field  $H$  created by electromagnet is applied perpendicularly to the wave vector  $q$ . External DC magnetic field  $H$  lies in the plane of sample either in parallel or in perpendicular to the vector of microwave electric field  $H_{\perp}$ . Microwave experiments were performed at the room temperature.

In the microwave experiments the modules of transmission  $D$  and reflection  $R$  coefficients and their relative change in the external magnetic field were measured  $d_m = [ |D(H)| - |D(0)| ] / |D(0)|$ , where  $|D(H)|$  is the transmission coefficient module in the magnetic field  $H$  and  $r_m = [ |R(H)| - |R(0)| ] / |R(0)|$ , where  $|R(H)|$  is the reflection coefficients module. In what follows, when considering the experimental results, for short, the transmission and reflection coefficients will be implied as their modules. Let us consider the magnetic field dependences of transmission and reflection coefficients for sample No.413/6-50 with  $\text{Fe}_3\text{Ni}_2$  nanoparticles. At first, the measurement results performed upon the standard disposition of fields, when the constant magnetic field  $H$  is perpendicular to

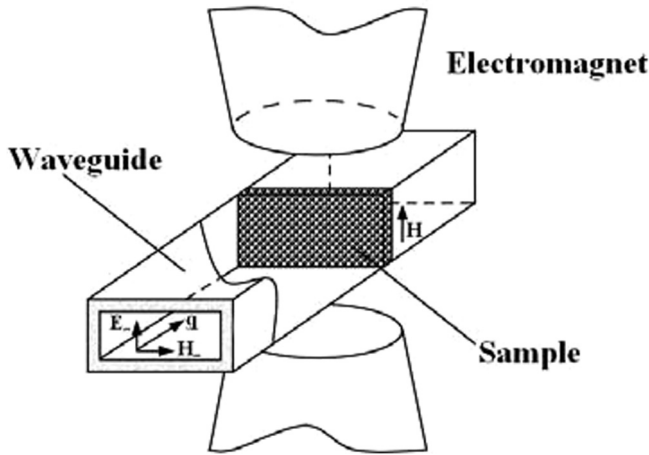


Fig. 4. Scheme of sample disposition in the waveguide.

microwaves magnetic field  $H_{\sim}$ ,  $H \perp H_{\sim}$ , are considered. These results are shown in Fig. 5.

The minima caused by uniform mode of ferromagnetic resonance are seen in the dependence of transmission coefficient. As usual, the minimum position is shifted toward higher fields when increasing the frequency. The maximum of transmission coefficient concerned with the antiresonance is not observed in this figure, anyhow, within the error of measurements of 0.4%. A similar pattern is observed in Fig. 5(b) for the reflection coefficient. The

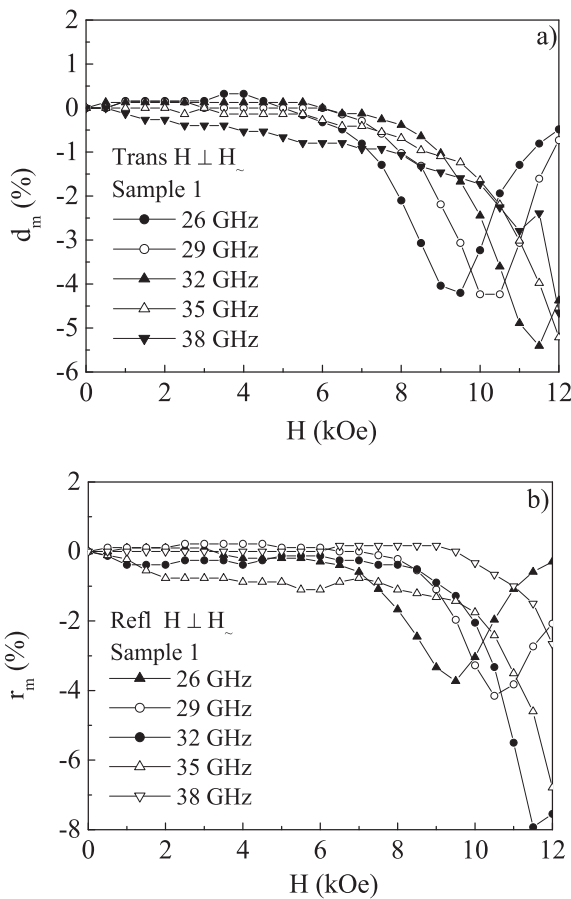


Fig. 5. The dependence of transmission (a) and reflection (b) coefficients for sample No.413/6-650 with  $Fe_3Ni_2$  nanoparticles. The constant magnetic field  $H$  is perpendicular to the microwave magnetic field  $H_{\sim}$ ,  $H \perp H_{\sim}$ .

minimum of reflection coefficient caused by FMR is clearly visible and the features of antiresonance are absent.

4.2. The results for parallel orientation of fields,  $H//H_{\sim}$ , are shown in Fig. 6. in this case, FMR in transmission is observed

The dependences of transmission and reflection coefficients on magnetic field intensity, measured at different frequencies ( $f$ ), allow one to reconstruct the spectra of magnetic resonance and antiresonance. At first, let us consider the spectra obtained for sample No.413/6-650 with  $Fe_3Ni_2$  nanoparticles (Fig. 7). These

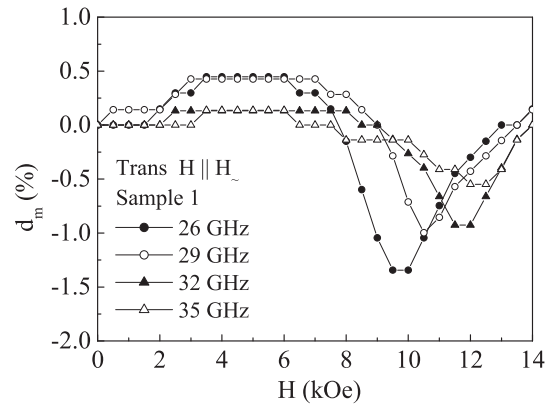


Fig. 6. The dependence of reflection coefficient for sample No.413/6-650 with  $Fe_3Ni_2$  nanoparticles. The constant magnetic field  $H$  is in parallel with the microwave magnetic field  $H_{\sim}$ ,  $H//H_{\sim}$ .

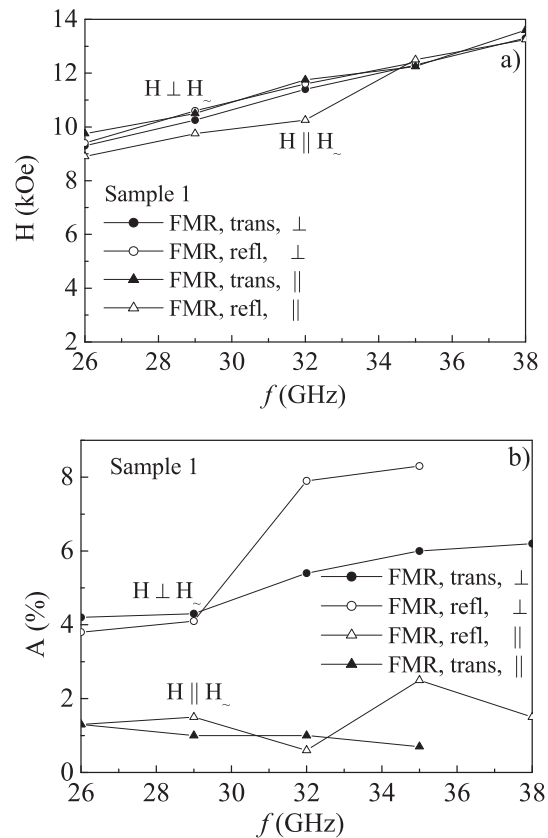
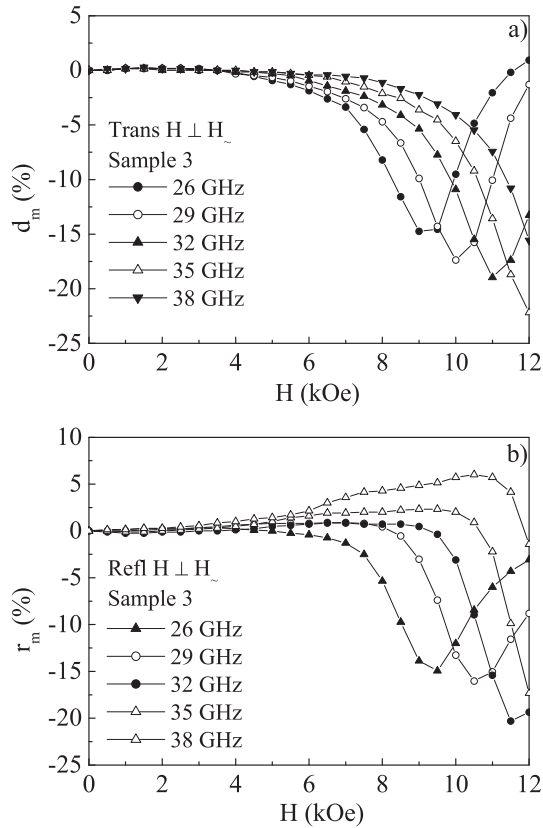


Fig. 7. The spectrum of magnetic resonance (a) and the frequency dependence of magnitude of lines of resonance changes of transmitted and reflected waves (b) for sample No.413/6-650 with  $Fe_3Ni_2$  nanoparticles.



**Fig. 8.** The dependence of transmission (a) and reflection (b) coefficients for sample No.414/6-650 with FeNi<sub>3</sub> nanoparticles. The constant magnetic field  $H$  is perpendicular to the microwave magnetic field  $H_{\perp}$ ,  $H \perp H_{\perp}$ .

spectra are reconstructed from experimental data of measurements of transmission and reflection coefficients.

The values of resonance fields measured at the same frequency but by using different methods are mostly close to each other, except for a few values obtained in reflection upon the parallel configuration of fields. Of course, for the broad resonance lines which are observed in these nanocomposites the true position of resonance only approximately coincides with the minimum of transmission or reflection coefficient.

After examination of spectra let us turn to the study of frequency dependence of magnitude of lines of resonances ( $A$ ). For the magnetic resonance which is pertinent to the uniform mode of precession when increasing the frequency an increasing of resonance line magnitude is a typical feature. The frequency dependence of magnitude of lines of resonance changes of transmitted and reflected waves for the same sample No.413/6-650 upon  $H \perp H_{\perp}$  is shown in Fig. 7(b). As expected, when increasing the frequency the magnitude of lines of FMR changes increases. For changes in the parallel orientation of fields  $H // H_{\perp}$  more complicated picture of changes is observed. Here, in reflection the magnitude of changes irregularly varies without clear tendency of rise of effect when increasing the frequency, whereas in transmission the magnitude of FMR lines decreases when increasing the frequency.

#### 4.3. Microwave resonance properties of the nanocomposite with FeNi<sub>3</sub> intermetallides

In this section the results of microwave measurements for samples with FeNi<sub>3</sub> nanoparticles are presented. The dependence of transmission and reflection coefficients for sample No.414/6-650 is shown in Fig. 8. Constant magnetic field  $H$  is perpendicular to

the microwave magnetic field  $H_{\perp}$ ,  $H \perp H_{\perp}$ . In the field dependences of transmission coefficient one can see FMR lines. The field of minimum increases when the frequency rises. This resonance corresponds to the uniform branch of FMR spectrum. In the field dependences of reflection coefficient both the resonance and antiresonance features are visible. The resonance is observed at all frequencies which are shown in figure and the maximum caused by antiresonance occurs only for 35 and 38 GHz. At lower frequencies the maximum is absent in compliance with well-known property of the magnetic antiresonance [13].

The data measured for parallel orientation of the fields,  $H // H_{\perp}$ , for the same sample are shown in Fig. 9. In contrast to the previous case, the maximum on the dependence of transmission coefficient on magnetic field is clearly visible. This maximum is visible at frequencies greater or equal to 32 GHz. In the field dependence of reflection coefficient the minimum caused by magnetic resonance is visible, but clear features of antiresonance are not observed. Abnormal changes of minimum magnitude should be noted. When increasing the frequency the minimum value decreases. This tendency is clearly visible both for reflection and for transmission of waves.

Let us consider the magnetic resonance and antiresonance spectra for sample No.414/6-650 with FeNi<sub>3</sub> nanoparticles. The spectra of FMR line, obtained upon the perpendicular orientation for transmission and reflection, as well as the spectrum obtained upon the parallel orientation in transmission are sufficiently close to each other. Let us perform the analysis of frequency dependence of magnitude of lines of resonance changes of transmitted and reflected waves, which are shown in Fig. 10(b).

For the magnitudes of FMR lines measured at  $H \perp H_{\perp}$  both for transmitted and reflected waves one can see a typical dependence

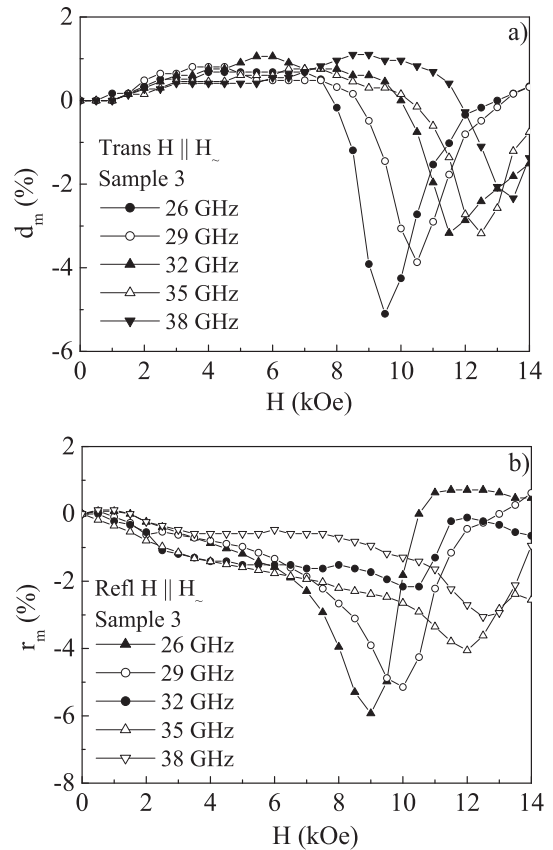


**Fig. 9.** The dependence of transmission (a) and reflection (b) coefficients for sample No.414/6-650 with FeNi<sub>3</sub> nanoparticles. The constant magnetic field  $H$  is in parallel with the microwave magnetic field  $H_{\perp}$ ,  $H // H_{\perp}$ .

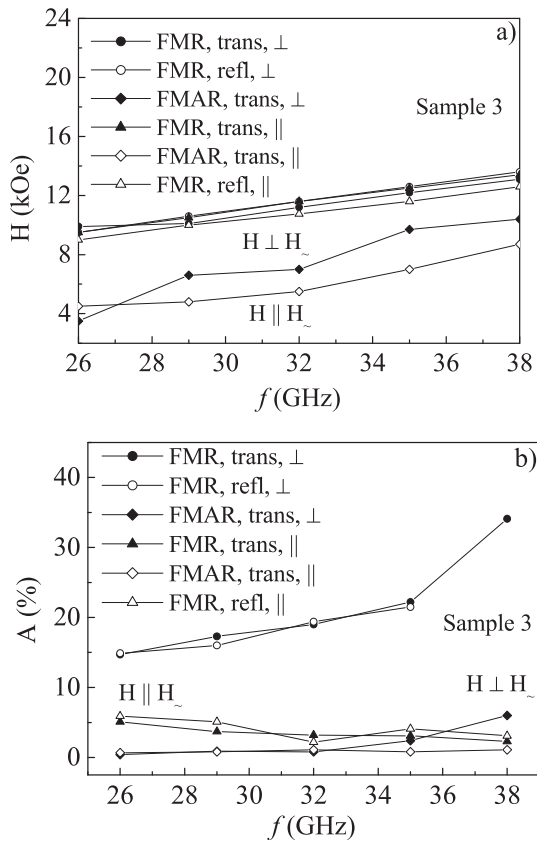


**Fig. 10.** The spectrum of magnetic resonance and antiresonance (a) and the frequency dependence of magnitude of lines of resonance changes of transmitted and reflected waves (b) for sample No.414/6-650 with FeNi<sub>3</sub> nanoparticles.

which increases when increasing the frequency. As it was mentioned above, the frequency dependence of magnitude of FMR lines upon  $H \parallel H_0$  has unusual character, i.e. the magnitude of FMR lines decreases when increasing the frequency.

The presence of the resonance changes upon  $H \parallel H_0$  is nontrivial and requires the explanations. It is well known [13] that for realization of FMR an existence of magnetization component which is perpendicular to the vectors of microwave magnetic field  $H_0$  is necessary. If the measurements are performed at sufficiently high frequencies and the field resonance turns out to be in the field of magnetic saturation then the magnetization direction is close to the external magnetic field direction. Then upon  $H \parallel H_0$  the condition  $M \parallel H_0$  approximately holds. In this case, the effective permeability is a component  $\mu_{33}$  of tensor of dynamic permeability, which don't suffers the changes of resonance type under FMR [13].

However, for the magneto-inhomogeneous media such as the nanocomposites based on opal matrices, the local direction of magnetization (for example, magnetization of individual ferromagnetic particle) can be significantly different from the direction of external field, except for full magnetic saturation. At lowest frequency of 26 GHz the resonance field is  $\sim 9$  kOe. According to Fig. 3 for the temperature of  $T = 300$  K this field corresponds to the region of magnetization curve which is close to saturation, but full saturation has not been reached. When increasing the frequency the position of resonance is shifted toward the stronger fields. At that the portion of particles having the perpendicular component of magnetization reduces. Therefore, when increasing the frequency the magnitude of lines of FMR should decrease.

Let us compare the values of FMR fields for the investigated samples. For example, at the frequency  $f = 26$  GHz the field of minimum ranges from 9 to 9.8 kOe for samples No.413/6-650 with

Fe<sub>3</sub>Ni<sub>2</sub> nanoparticles, and No.414/6-650 with FeNi<sub>3</sub> nanoparticles for all version of measurements upon  $H \perp H_0$ . According to the Kittel formula [13] an approximate equality of resonance fields for different samples of the same shape signifies approximate equality of magnetization of samples. However, this experimental fact is in contradiction with the results of magnetic measurements which are shown in Fig. 3 and summarized in Table 1. The magnetization of nanocomposite in the samples No. 413/6-650 with Fe<sub>3</sub>Ni<sub>2</sub> nanoparticles is 4.01 emu/g, and in the sample No. 414/6-650 with FeNi<sub>3</sub> nanoparticles are 15.21 emu/g. The apparent contradiction is solved taking into account that the frequency of FMR for magnetically inhomogeneous sample is determined by the particles or layers magnetization of ferromagnetic phase, rather than by the average (effective) magnetization of entire sample. Thus, the difference in saturation magnetization of these samples (Table 1) is in the first place caused by the magnetic phase concentration in the samples rather than by the difference of magnetization of ferromagnetic phase themselves.

## 5. Conclusions

The magnetic and microwave properties of 3D nanocomposites based on the opal matrices with the nanoparticles of Fe-Ni intermetallics, namely, Fe<sub>3</sub>Ni<sub>2</sub> and FeNi<sub>3</sub>, which are embedded into the interspherical voids, have been studied in this paper. The phenomena of magnetic resonance and antiresonance for two orientations of external magnetic field have been studied in detail. It has been shown that FMR line relating to the uniform branch of spectrum exists not only upon the perpendicular orientation of constant and microwave magnetic fields,  $H \perp H_0$ , but also upon the parallel orientation,  $H \parallel H_0$ . The presence of resonance in the parallel orientation is caused by magnetic heterogeneity of sample. The spectra of magnetic resonance and antiresonance in nanocomposites containing the particles of Fe<sub>3</sub>Ni<sub>2</sub> and FeNi<sub>3</sub> intermetallics have been studied. The investigation of frequency dependence of magnitude of lines of magnetic resonance yield important result. The magnitude of FMR line in nanocomposites upon the parallel orientation of fields  $H \parallel H_0$  decreases when increasing the frequency. This abnormal dependence is caused by the shift of FMR field close to the magnetic saturation when increasing the frequency.

In the samples with large portion of ferromagnetic phase and with high magnetization of nanocomposite the magnitude of lines of resonance changes amounts tens of percents. The results obtained predetermine the development of microwave devices controlled by magnetic field.

## Acknowledgments

The work is carried out within the RAS program "Spin" No 01.2.006 01201463330, with partial support of grant from Russian Ministry of Education and Science No 14.Z50.31.0025.

## References

- [1] A.K. Sarychev, V.M. Shalaev, *Electrodynamics of metamaterials*, World Scientific and Imperial College Press, 2007, p. 200.
- [2] Fuxi Gan, Lei Xu, *Photonic glasses*, Imperial College Press, 2006, p. 460.
- [3] A.B. Rinkevich, D.V. Perov, M.I. Samoylovich, S.M. Klescheva, V.O. Vaskovsky, *Microwave and magnetic properties of cobalt-containing magnetophotonic crystals*, in: Yamato Kobayashi, Haruto Suzuki (Eds.), *Cobalt: Occurrence, uses and Properties*, Nova Science Publishers, New York, 2013, pp. 1–60, Chapter 1.
- [4] E. Ozbay, B. Temelkuran, M. Bayindir, *Microwave applications of photonic crystals*, *Progr. Electromagn. Res.* 4 (2003) 185–209.
- [5] Richard W. Ziolkowski, Ehud Heyman, *Wave propagation in media having negative permittivity and permeability*, *Phys. Rev. E* 64 (1-15) (2001) 056625.
- [6] A.B. Rinkevich, D.V. Perov, S.O. Demokritov, M.I. Samoylovich, O.V. Nemytova, *Interaction of microwave electromagnetic waves with 3d magnetic metamaterials*, *Photonics Nanostruct. Fundam. Appl.* 15 (2015) 59.

- [7] M.G. Silveirinha, N. Engheta, Tunneling of electromagnetic energy through sub-wavelength channels and bends using epsilon-near-zero (ENZ) materials, *Phys. Rev. Lett.* 97 (2006) 4 pages 157403.
- [8] M.G. Silveirinha, N. Engheta, Tunneling of electromagnetic energy through sub-wavelength channels and bends using epsilon-near-zero (ENZ) materials, *Phys. Rev. Lett.* 97 (2006) (4 pages) 157403.
- [9] R.W. Ziolkowski, Propagation in and scattering from a matched metamaterial having a zero index of refraction, *Phys. Rev. E* 70 (4) (2004) 046608(12).
- [10] C.R. Alves, R. Aquino, J. Depeyrot, F.A. Tourinho, E. Dubois, R. Perzynski. Superparamagnetic relaxation evidences large surface contribution for the magnetic anisotropy of MnFe<sub>2</sub>O<sub>4</sub> nanoparticles of ferrofluids, in: 4th Brazilian MRS Meeting, February 2007.
- [11] Su Hua, Zhang Huaiwu, Tang Xiaoli, Liu Yingli, Effects of nanocrystalline ferrite particles on densification and magnetic properties of the NiCuZn ferrites, *J. Mater. Sci.* 42 (2007) 2849–2853A.
- [12] K.D. Usadel, Temperature-dependent dynamical behavior of nanoparticles as probed by ferromagnetic resonance using Landau-Lifshitz-Gilbert dynamics in a classical spin model, *Phys. Rev. B* 73 (2006) 212405.
- [13] A.G. Gurevich, G.A. Melkov, *Magnetization Oscillations and Waves*, CRC Press, Boca Raton, 1996.
- [14] B. Heinrich, V.F. Mescheryakov, Transmission of electromagnetic wave through ferromagnetic metal near antiresonance, *ZhETPh Lett.* 9 (1969) 618–622 (in Russian).
- [15] M.I. Kaganov, Excitation of standing spin waves in a film, *Sov. Phys. JETP.* 12 (1) (1960) 114.
- [16] H. Garcia-Miquel, S.M. Bhagat, S.E. Lofland, G.V. Kurl'yanskaya, A.V. Svalov, Ferromagnetic resonance in FeCoNi electroplated wires, *J. Appl. Phys.* 94 (3) (2003) 1868–1872.
- [17] D.L. Mills, R.E. Camley, Theory of microwave propagation in dielectric/magnetic film multilayer structures, *J. Appl. Phys.* 82 (6) (1997) 3059–3067.
- [18] Lucía Fernández-García, Marta Suárez, Jose Luis Menéndez, Carlos Pecharrromán, Ramón Torrecillas, Pavel Y Peretyagin, Jan Petzelt, Maxim Savinov, Zdenek Frait, Antiresonance in (Ni, Zn) ferrite-carbon nanofibres nanocomposites, *Mater. Res. Express* 2 (2015) 1–6 055003.
- [19] V.V. Ustinov, A.B. Rinkevich, D.V. Perov, M.I. Samoilovich, S.M. Klescheva, Anomalous magnetic antiresonance and resonance in ferrite nanoparticles embedded in opal matrix, *JMMM* 324 (1) (2012) 78–82.
- [20] V.V. Srinivasu, S.E. Lofland, S.M. Bhagat, K. Ghosh, S.D. Tyagi, Temperature and field dependence of microwave losses in manganite powders, *J. Appl. Phys.* 86 (1999) 1067.
- [21] A.B. Rinkevich, M.I. Samoilovich, S.M. Klescheva, D.V. Perov, A.M. Burkhanov, E. A. Kuznetsov, Millimeter-wave properties and structure of gradient Co-Ir Films deposited on opal matrix, *IEEE Trans. Nanotechnol.* 13 (1) (2014) 3–9.
- [22] D.E. Endean, J.N. Heyman, S. Maat, E.D. Dahlberg, Quantitative analysis of the giant magnetoresistance effect at microwave frequencies, *Phys. Rev. B* 84 (21) (2011) 1–4 212405.
- [23] A.B. Rinkevich, A.M. Burkhanov, M.I. Samoilovich, A.F. Belyanin, S.M. Kleshcheva, E.A. Kuznetsov, Three-dimensional nanocomposite metal dielectric materials on the basis of opal matrices, *Russ. J. Gen. Chem.* 83 (11) (2013) 2148–2158.
- [24] Mitsuteru Inoue, Magnetophotonic crystals, in: *Proc. MRS, Symposium J, "Magneto-Optical Materials for Photonics and Recording"*, Boston. November 2004.
- [25] S.V. Vonsovsky, *Magnetism*, vol. 2, John Wiley, New York, 1974.
- [26] Harun Bayrakdar, Complex permittivity, complex permeability and microwave absorption properties of ferrite-paraffin polymer composites, *JMMM* 323 (2011) 1882–1885.